JOURNAL OF GEOPHYSICAL RESEARCH, VOL. 102, NO. C7, PAGES 15,679–15,691, JULY 15, 1997

Dependence of apparent optical properties on solar altitude: Experimental results based on mooring data collected in the Sargasso Sea

Malgorzata Stramska

Hancock Institute for Marine Studies, University of Southern California, Los Angeles

Daniel Frye

Woods Hole Oceanographic Institution, Woods Hole, Massachusetts

Abstract. The in situ variability of the vertical attenuation coefficient for downward irradiance (K_d) and radiance reflectance (R_L) in response to changing solar altitude has been investigated. Observations were made 18 times per day from a fixed position mooring deployed in the Sargasso Sea. The mooring included instrumentation to measure spectral downwelling irradiance (E_d) and spectral upwelled radiance (L_u) at 15- and 35-m depths. Time series data used for our analysis represent conditions of low, almost constant concentration of chlorophyll-like pigments in the water and sunny or partly cloudy sky conditions. During sunny days the dominant component of the observed diel variability of the apparent optical properties (AOPs) was caused by the variable solar altitude. The statistical analysis performed on the data indicates a significant correlation between K_d and the cosine of the zenith angle of the direct solar beam after refraction at the air/water boundary (μ). These changes were wavelength dependent; K_d at 412, 443, 490, 510, and 555 nm decreased by 18-30%, while K_d at 665 and 683 nm increased by more than 50% when solar altitude increased from about 17° to 60° (i.e., when μ increased from 0.69 to 0.93). The vertical attenuation coefficient for photosynthetically available radiation (K_{PAR}) decreased by about 25%. The daily amplitudes of similar changes in R_L at the blue/green light were much smaller, up to about 4 to 8% at 412, 443, 490, and 510 nm and 11% at 555 nm. However, at 665 and 683 nm, R_L changed by more than 100%. This large increase of R_L and decrease of K_d at 665 and 683 nm with Sun altitude (with μ) can be explained by the fact that the light field at red wavelengths was strongly affected by inelastic processes such as Raman scattering and natural fluorescence. Remote-sensing techniques rely on the interpretation of reflectance and upwelled radiance ratios. We observed up to 8% changes in reflectance ratios and up to 17% changes in upwelling radiance ratios during the day. These maximum changes were observed for the ratios including L_u or R_L at 555 nm, which were affected by inelastic scattering of light. Although our data illustrate the dependence of AOPs on the Sun altitude on a daily timescale, similar relationships are expected to be of importance on a seasonal scale and with latitude.

Introduction

Remote-sensing techniques have vastly enhanced our capabilities to determine phytoplankton biomass, primary production, and carbon cycling in the ocean and increased our understanding of their temporal and spatial variability. Light emanating from the surface of the ocean contains a wealth of information regarding absorption and scattering properties of the water and its particulate and dissolved constituents. However, the spectral signal received by a satellite is a complex function of optical processes in the atmosphere, air-sea interface, and upper ocean. The ability to predict in-water constituent concentrations from a satellite depends on the ability to separate the signal variability affected by these constituents from the signal variability related to other processes.

Paper number 97JC00886.
0148-0227/97/97JC-00886$09.00

To characterize oceanic waters, optical oceanographers commonly use apparent optical properties (AOPs) such as the vertical attenuation coefficient for downward irradiance (K_d) and radiance reflectance (R_L). Recall that $R_L = L_u/E_d$, where L_u is the radiance directed vertically upward and E_d is the downward irradiance, both measured at the same depth (z). The attenuation coefficient K_d is defined as $K_d = 1/E_d\ [dE_d/dz]$ (see, e.g., Kirk [1994a] for definitions of optical quantities). This use of apparent properties involves the "quasi-inherency approximation", assuming the independence of these properties with respect to the in situ geometry of the radiance distribution [*Baker and Smith*, 1979]. This is in agreement with observations showing that vertical attenuation coefficient and reflectance are strongly correlated with inherent optical properties (IOPs) and can provide a useful connection between ocean optics and biology. Inverse radiative transfer modeling has lead to several relationships that can be used to estimate IOPs of oceanic water such as the absorption (a), scattering (b), and beam attenuation (c) coefficients from the measured AOPs [e.g., *Gordon et al.*,

1975; *Jerlov*, 1976; *Morel and Prieur*, 1977; *Smith and Baker*, 1982; *Gordon and Morel*, 1983; *Kirk*, 1994a, b, c]. This approach is very attractive because apparent optical properties are more easily measured in situ than inherent optical properties.

However, quasi-inherency of AOPs is only an approximation, and in general, the AOPs are influenced by the angular structure of the light field. Therefore the AOPs are expected to vary with, for example, changes in the proportion of the direct and diffuse solar radiation coming from the atmosphere and the state of the sea surface [e.g. *Gordon et al.*, 1975; *Jerlov*, 1976]. One of the most important factors influencing AOPs is the variability of solar altitude. The nature of this dependency has been investigated recently through Monte Carlo computer simulations [*Kirk*, 1984. 1991; *Gordon*, 1989; *Morel and Gentilli*, 1991, 1993].

The most important goal of this paper is to investigate the in situ variability of AOPs such as the vertical attenuation coefficients for downward irradiance (K_d) and radiance reflectance (R_L) in response to changing solar altitude. Note that in general it may not be an easy task to collect data which would allow quantifying such variability. For example, optical data are typically collected by instruments lowered from ships. This type of data is limited in temporal resolution as well as by errors due to the ship movements and shadowing. Our data are not affected by such errors, because the observations were made 18 times per day with spectral radiometers deployed on the fixed position mooring. Importantly, our time series data were collected during conditions of almost constant concentration of chlorophyll-like pigments in the surface waters; therefore it is reasonable to believe that the dominant component of the diel variability in the

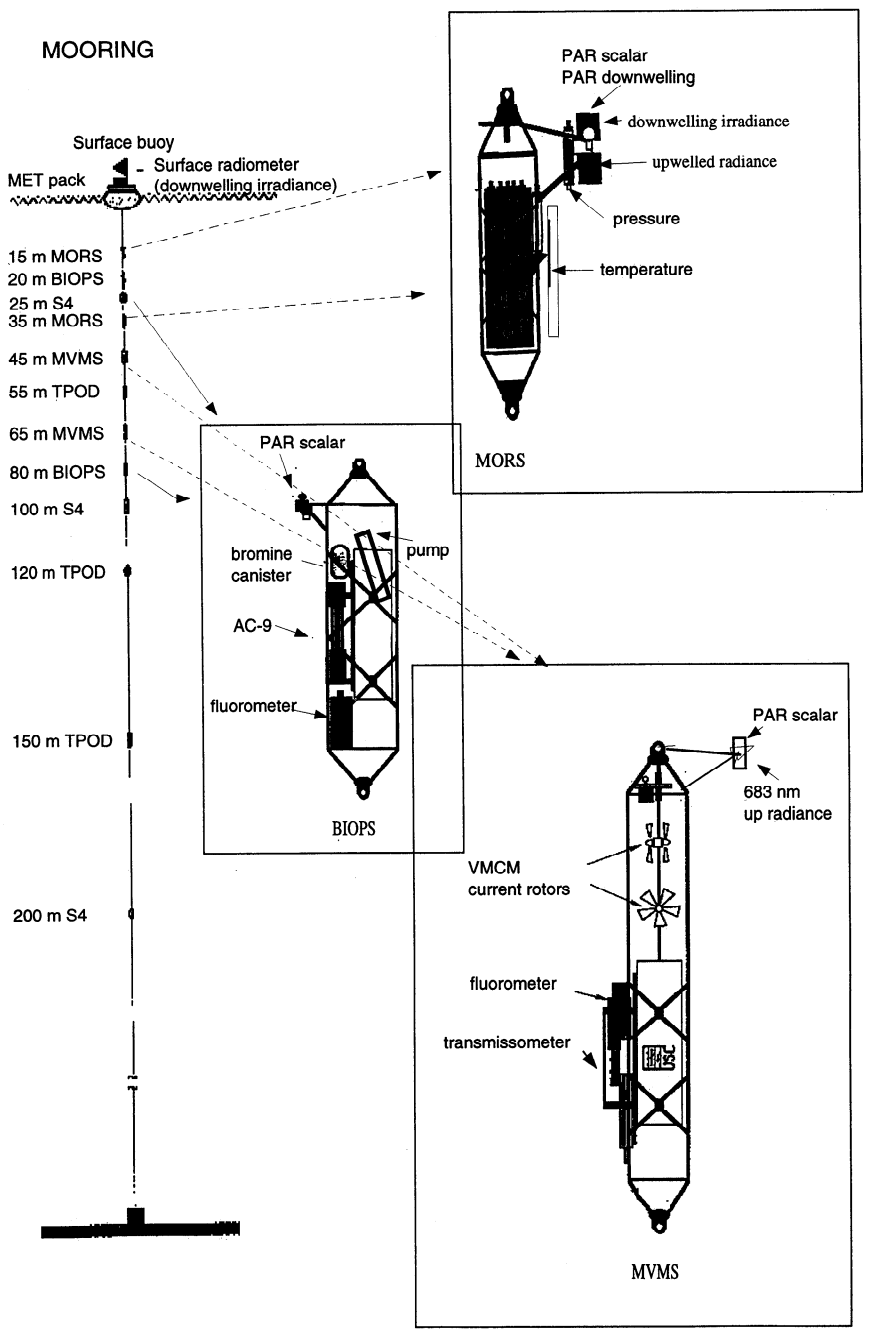

Figure 1. Configuration of the mooring deployed near Bermuda in September 1994.

apparent optical properties was caused by the daily changes of Sun elevation.

Methods

The data presented in this paper were collected from a mooring located about 80 km southeast off Bermuda in waters of ~ 4570-m depth. This location for the testbed mooring was selected because it is near the Bermuda Atlantic Time Series Study (BATS) site, which has been regularly sampled since October 1988, during monthly/biweekly R/V *Weatherbird II* cruises [*Michaels et al.*, 1994; *Siegel et al.*, 1995]. The BATS data show that the site is representative of major oligotrophic gyres. The region is characterized by occasional mesoscale variability and by the dominant seasonal scale [*Michaels et al.*, 1994].

The design of the mooring deployed in September 1994 is shown in Figure 1. The mooring included the following instrumentation:

On the surface buoy, there were instruments to measure wind speed and direction and air temperature (Coastal Climate), spectral downwelling irradiance (Satlantic), downwelling photosynthetically available radiation (PAR) (400-700 nm, Li-cor), and X and Y tilt sensors.

At 15- and 35-m depths, there were radiometer packages (MORS) with spectral downwelling irradiance and upwelled radiance sensors (Satlantic), scalar and downwelling PAR sensors (Li-cor), and water temperature and pressure sensors (Sea-Bird).

At 20- and 80-m depths, there were bio-optical sensor packages (BIOPS), each with nine-wavelength absorption/attenuation meter (AC-9, WET Labs), stimulated fluorometer (SeaTech), and scalar PAR sensor (Biospherical).

At 45- and 65-m depths, there were multivariable moored systems (MVMS), each including a vector measuring current meter (VMCM), a thermistor for water temperature measurements, a scalar PAR sensor (Biospherical), a beam transmissometer (660 nm), and a stimulated fluorescence sensor (both from SeaTech). The MVMS has been described in several papers [e.g., *Dickey et al.*, 1994; *Stramska et al.*, 1995].

Additionally, there were three water temperature recorders (TPODS) at 55-, 120- and 150-m depths, nitrate analyzers at 80- and 200-m depth, and S-4 current meters at 25 and 200 m.

Data collected with the MORS radiometers at 15 and 35 m are the main focus of this article. For comparison, some of the data collected with other instruments will also be shown. The basic instruments in the MORS packages, Satlantic radiometers OCI-100 and OCR-200, comply, according to the manufacturer specifications, with the sea-viewing wide field-of-view sensor (SeaWiFS) requirements [*Mueller and Austin*, 1992; *Mueller et al.*, 1993]. The radiometers measured downwelling irradiance and upwelled radiance at seven 10-nm bandwidths centered at 412, 443, 490, 510, 555, 665, and 683 nm. The selection of the measured wavelengths makes it possible to evaluate bio-optical models in terms of the quantities available from satellite ocean color sensors. As mentioned above, the sensor suite also

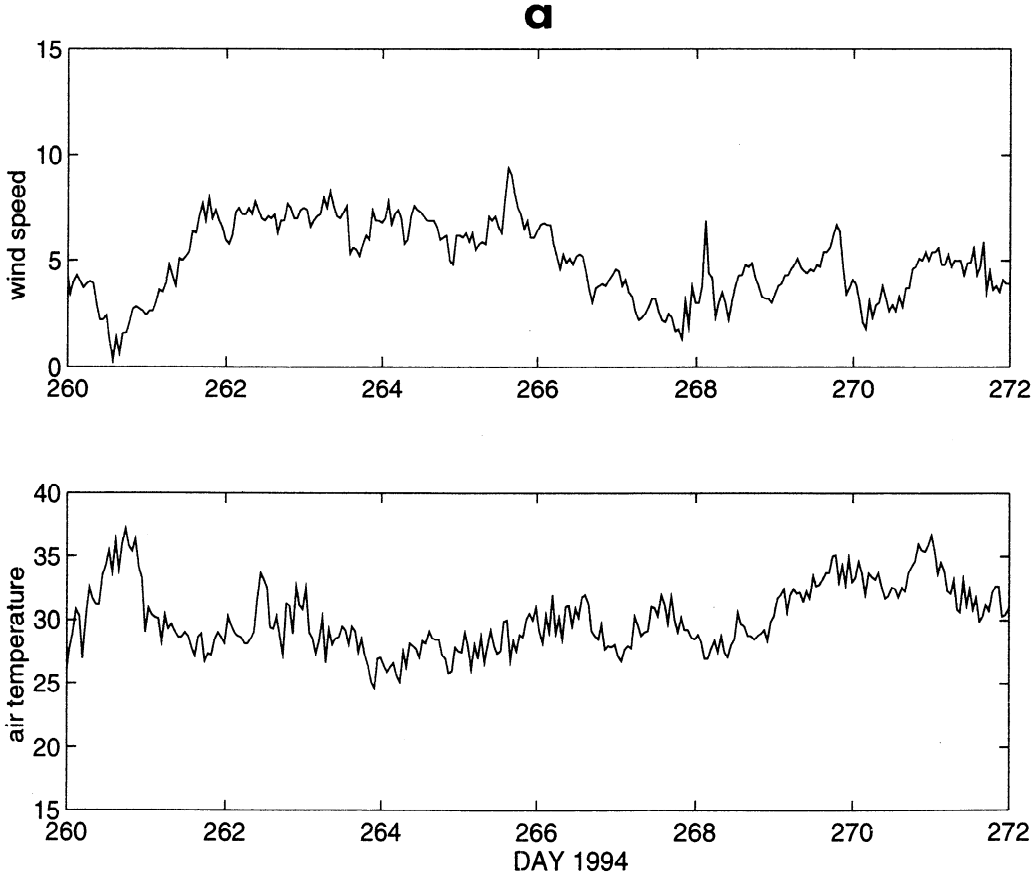

Figure 2. (a) Time series of wind speed (m s^{-1}) and air temperature (^{o}C). (b) Time series of PAR (μEinst $m^{-2}s^{-1}$), stimulated fluorescence (fluo, mg chl *a* m^{-3}) at 20-, 45-, 65-, and 80-m depths, and chlorophyll absorption (m^{-1}) at 20- and 80-m depths.

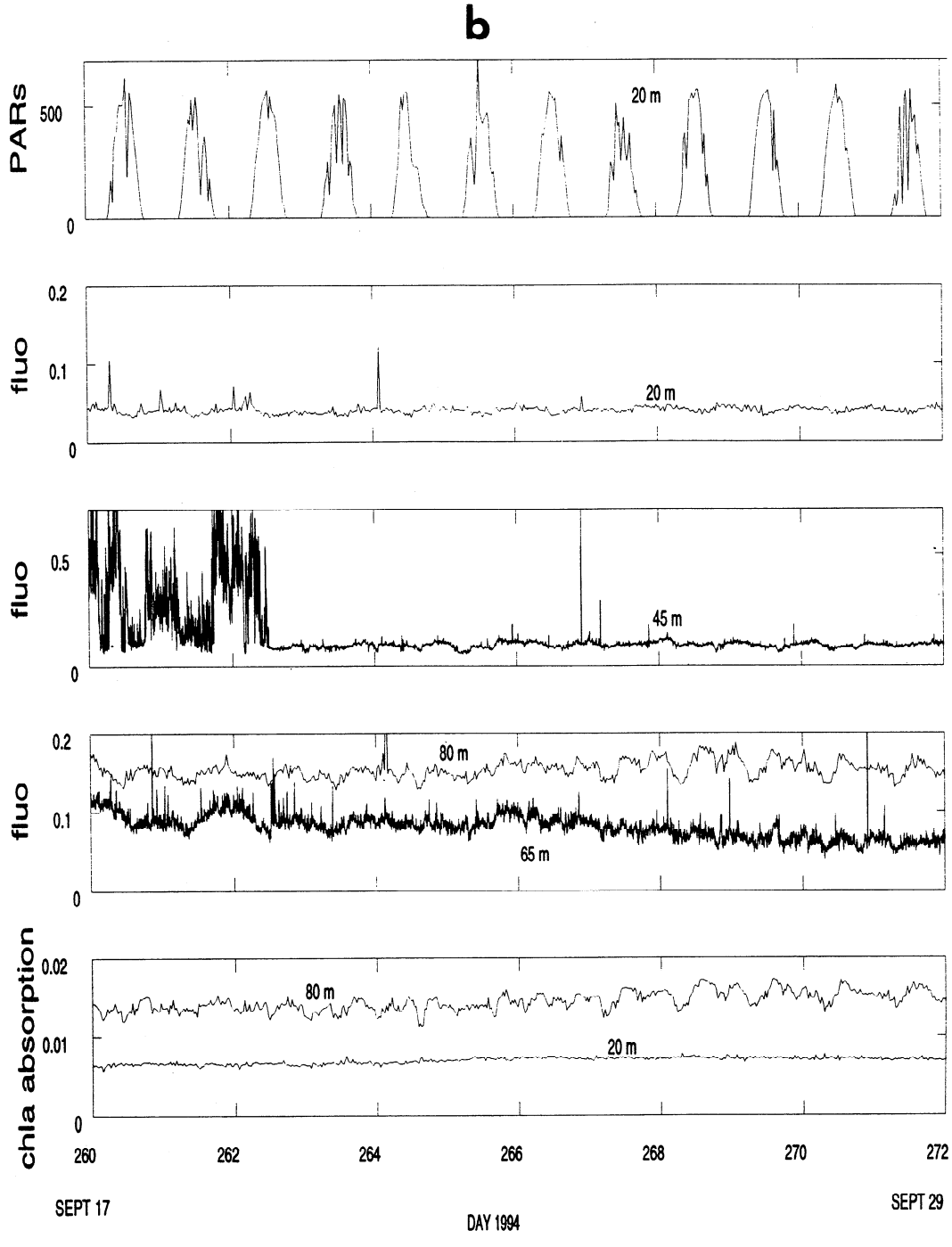

Figure 2. (continued)

included scalar and downwelling PAR sensors (calibrated for underwater measurements) and water temperature and pressure sensors. Mechanical installation of the light sensors was designed in such a way that the effect of shading was minimized (Figure 1). Sensor heads were mounted on the upper part of the instrument cage, to which a special arm was added, extending 30 cm away from the cage. The length of this arm represents a compromise between minimizing possible contamination of the data by shading and the logistical requirement of mooring deployment and recovery operations.

All the parameters, except water temperature, were sampled once every hour from 0900 to 2300 UT (0600 to 0800 LT in Bermuda), over a sampling time of 2 or 5 min, and at a rate of 6 Hz. Because of the limited memory of the data acquisition system the 5-min time series were collected only at 1400, 1500 and 1600 UT (near local noon). For the evaluation of possible sensor drift, data were also collected three times at night. Sampling periods of a few minutes were chosen to allow for averaging of the radiometric data over high frequency variability related to surface wave focusing effects [e.g., *Dera and Gordon,* 1968], changing conditions due to passing clouds, and changes in depths due to surface waves, tides, and mooring oscillations. On the other hand, these 2- and 5-min time series can be regarded as stationary with regard to solar altitude. Water temperature was

measured once every 15 min. The data were recorded with full frequency resolution (6 Hz for radiometric and pressure data) using internal hard drives on the in situ system, downloaded after the recovery of the mooring and averaged.

In addition to the MORS data, some of the data collected with BIOPS systems will be presented. The BIOPS sensor package included the AC-9 [*Zaneveld et al.*, 1992], a stimulated fluorometer, and a sensor for scalar irradiance PAR. The AC-9 measured inherent optical properties: the absorption (a) and attenuation (c) coefficients at nine wavelengths (412, 440, 488, 520, 560, 630, 650, 676, and 715 nm). A schematic of the mechanical mounting of the sensors on the package is shown in Figure 1. The AC-9 was mounted vertically, with a bromine canister above it, as suggested by the manufacturer. The bromine flushing system was used to minimize biological fouling. The bromine solution diffused through the AC-9 tubes when the unit was not acquiring data. When power was applied to the system, a pump flushed AC-9 tubes with fresh seawater. To flush the system, the AC-9 and the water pump were turned on 20 s prior to the start of data acquisition; then the data were collected for ~20 s, with a 6-Hz sampling rate. The AC-9 data were collected once every half hour. All raw data were recorded on the hard drive and downloaded and processed after mooring recovery.

Unfortunately, the analysis of the processed data has led us to the conclusion that the AC-9 data from this test deployment were generally of poor quality, probably because of biofouling. We observed that the signal for $a(\lambda)$ and $c(\lambda)$ increased continuously in time, most rapidly at short wavelengths. Therefore in this paper we will not consider the absorption spectrum. Instead, we will refer only to the "chlorophyll absorption" which has been estimated by examining the relative height of the red absorption peak in the absorption spectrum. This has been done in accordance with the following expression: $a_{chl} = (a_{676} - a_{w676}) - (a_{715} - a_{w715})$, where a_w represents the absorption of pure water. Such interpretation of the AC-9 data follows the procedure used for the AC-3, an earlier version of the absorption/attenuation meter, which measured $a(\lambda)$ and $c(\lambda)$ at three wavelengths and internally calculated the height of the red absorption peak. This treatment of the AC-9 data is further justified because we will consider here the time variability of the chlorophyll concentration during the first 12 days of the deployment when biofouling was still modest.

Finally, we will also show some of the time series data recorded by stimulated fluorometers at 20-, 45-, 65-, and 80-m depths. All fluorometers used during this experiment were calibrated in the laboratory before the deployment. The

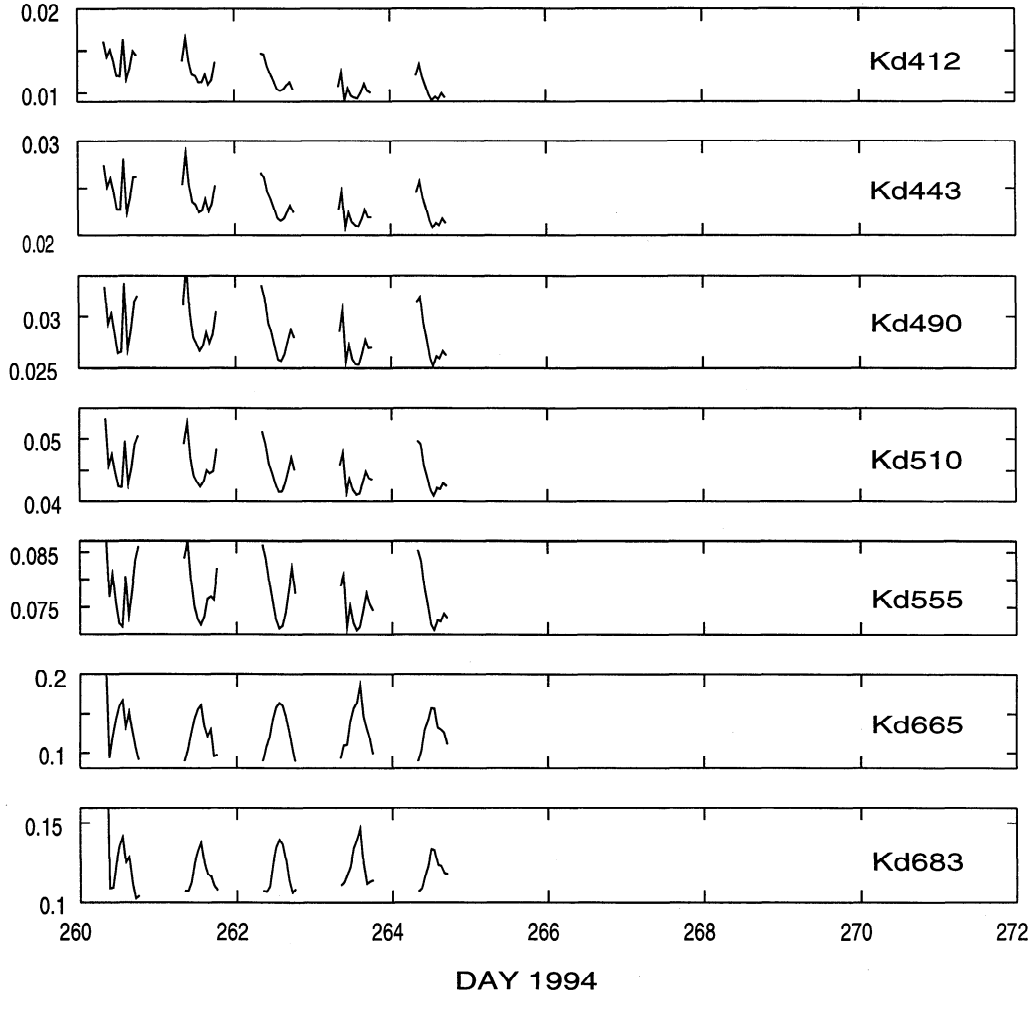

Figure 3. Time series of vertical attenuation coefficient for downwelling irradiance (K_d, m^{-1}) at seven wavelengths (412, 443, 490, 510, 555, 665, and 683 nm).

calibration was done by comparison of the fluorometer voltage with the concentration of the chlorophyll-like pigments in the phytoplankton (diatom) culture. This concentration was estimated using a spectrophotometric method with water samples passed onto GF/F filters and cold extracted for 24 hours in 90% acetone. It should be noted that the conversion of fluorometer data from volts to chlorophyll *a* (chl *a*) in situ is affected by factors such as phytoplankton species composition and physiological state [e.g., *Kiefer and Reynolds*, 1992]. However the calibration, even if not very exact, enables a comparison of the output from the instruments located at different water depths.

Results and Discussion

An overview of the conditions at the mooring site from September 17 to 28, 1994 (year days 260-271), is presented in Figure 2. Time series of wind speed and air temperature are

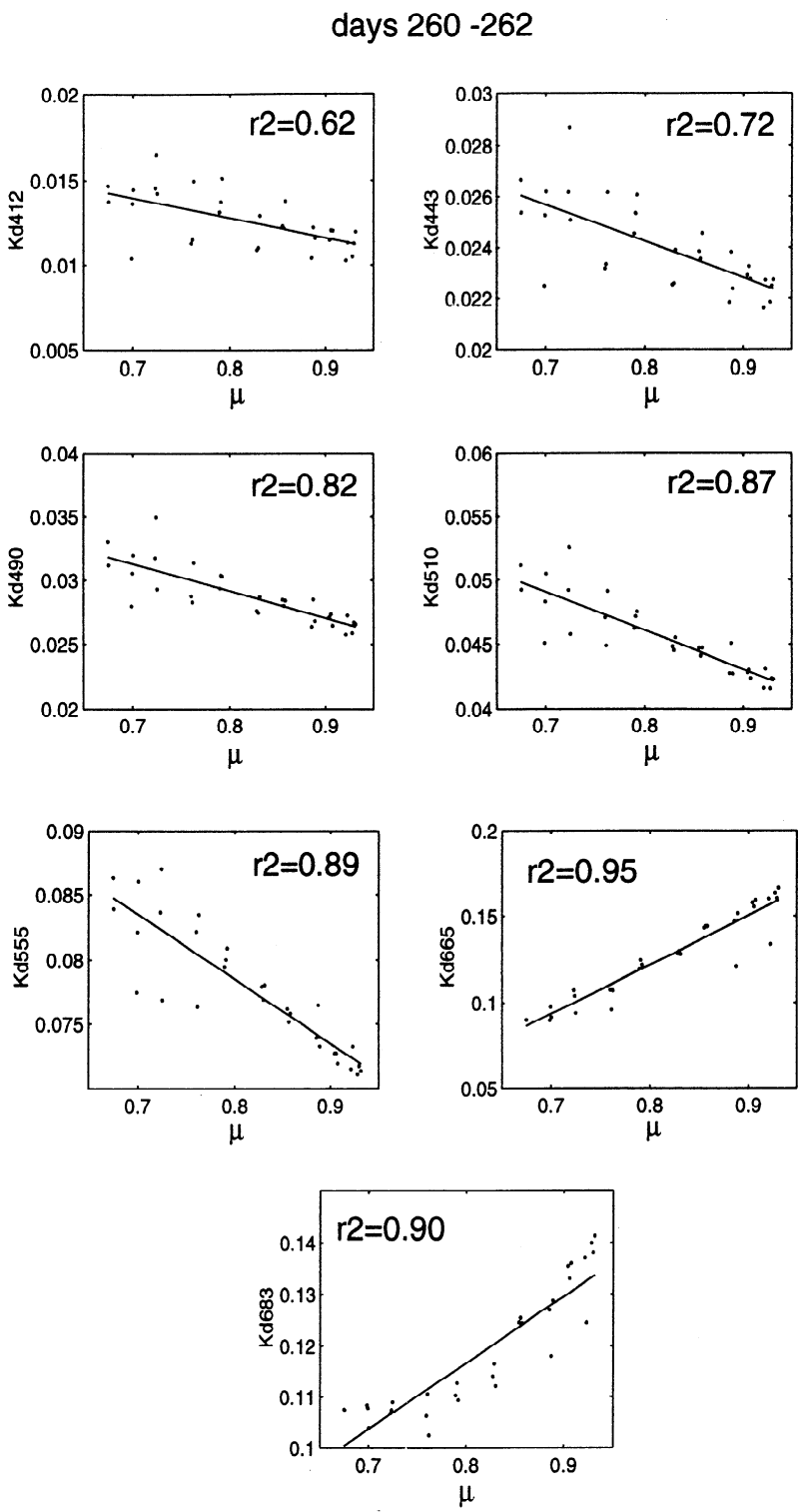

Figure 4. The dependence of the vertical attenuation coefficient for downwelling irradiance (K_d, m^{-1}) on the cosine of the refracted zenith angle of the direct solar beam (μ).

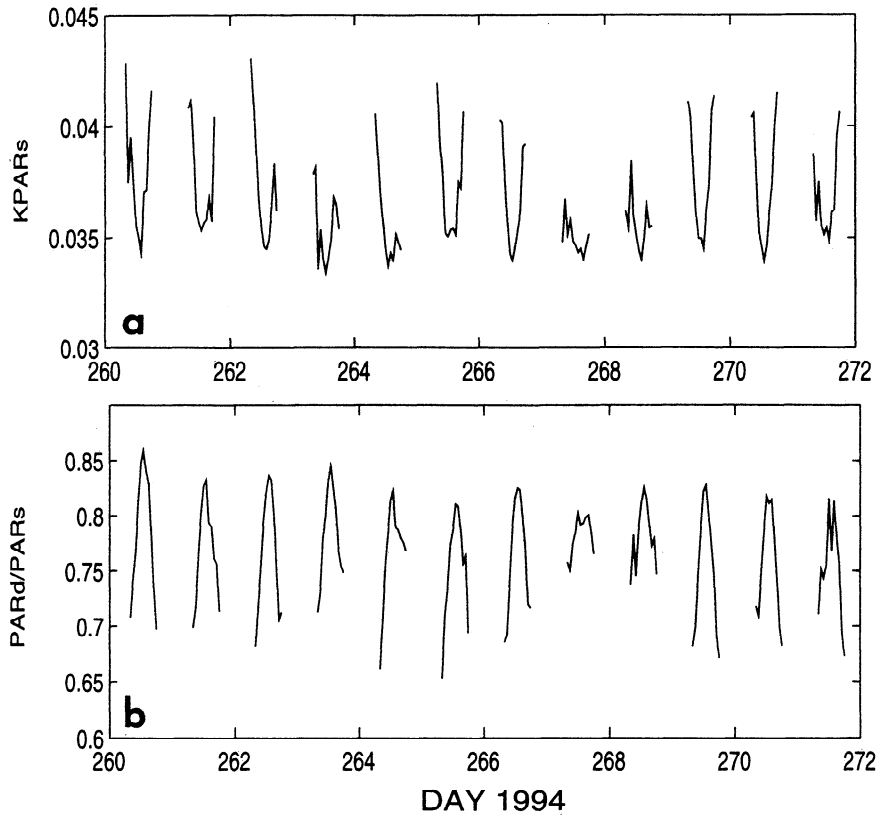

Figure 5. Time series of (a) K_{PAR} (m^{-1}) and (b) the PAR_d/PAR_s ratio at 15-m depth.

shown in Figure 2a. This time period was characterized by weak and moderate winds (< 8 m/s) and air temperature was in the range of 25-37 °C. Time series of the water temperature (not shown here) indicated relatively strong thermal stratification. The 20-m PAR time series data shown in the top panel of Figure 2b indicate that sunny and partly cloudy sky conditions prevailed. Time series of stimulated fluorescence at 20-, 45-, 65-, and 80-m depths and chlorophyll absorption estimated from AC-9 measurements at 20- and 80-m depths are also shown in Figure 2b. These measurements indicate very low, almost constant concentrations of chlorophyll-like pigments in surface water. Somewhat higher concentrations, but not exceeding 0.6 mg chl *a* m^{-3}, were observed only on days 260-262 at 45-m depth. This is in agreement with the conductivity-temperature-depth (CTD), beam attenuation, and fluorescence profiles done from *Weatherbird II* just before and after the deployment of the mooring, during the night (259/260), which indicated the chlorophyll maximum to be at 40-50 m.

From the time series of downwelling spectral irradiance measured at 15 and 35 m we estimated vertical attenuation coefficients, K_d. These time series of K_d estimated at seven wavelengths are shown in Figure 3. Unfortunately, because the 35-m radiometer failed after 5 days, our time series for K_d are much shorter than the 15-m reflectance time series discussed later (Figure 7). Nevertheless, to facilitate the comparison between Figures 2, 3, and 7, the horizontal scale in Figure 3 extends from day 260 to 271. During the initial 5-day time period, phytoplankton concentration in the surface waters was relatively

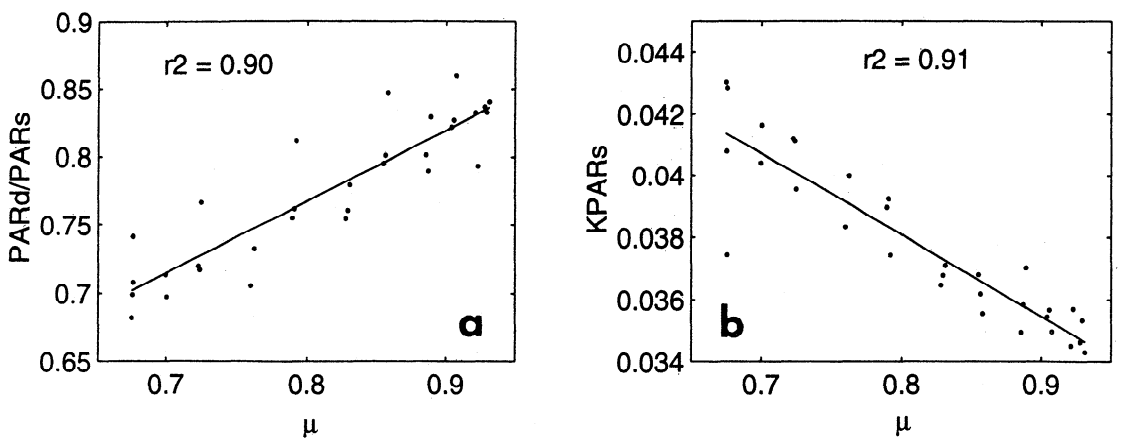

Figure 6. (a) PAR_d/PAR_s ratio at 15-m depth and (b) K_{PARs} (m^{-1}) as a function of μ.

constant (see Figure 2). Somewhat variable phytoplankton concentration at 45 m should not have a significant effect on the K_d estimated from irradiance measured at 15- and 35-m depths. In Figure 3 one can observe the diel cycle in K_d, which is especially pronounced at times when clear sky conditions prevailed (compare with PAR time series, Figure 2). Note that the pattern of daily changes in K_d for red wavelengths (665 and 683 nm) is quite the opposite of that observed for all the other wavelengths; that is, maxima of K_d are observed at noon for 665 and 683 nm.

To better illustrate this dependency, the data points from Figure 3 are replotted in Figure 4 as a function of the cosine of the zenith angle of the direct solar beam in water, μ. Photons incident on the sea surface undergo refraction at the air/water boundary in accordance with Snell's law [e.g., *Kirk*, 1994a]; therefore the cosine of the zenith angle of the direct solar beam after refraction is a better choice for our correlation than a solar zenith angle in the air. Note that because our measurements were made in September, maximum solar altitude in Bermuda during the day was about 60°, which corresponds to a solar zenith angle of 30°, a refracted solar zenith angle of 21.9°, and a μ of about 0.93.

It can be seen from Figure 4 that as μ increased (solar altitude increased), the value of the vertical attenuation coefficient changed, and this dependency has been approximated with the linear relationship. Such changes were wavelength dependent, as mentioned above. Note first that K_d at 412, 443, 490, 510, and 555 nm decreased by 18% to 30% when the solar altitude increased from about 17° to 60° (when μ increased from about 0.69 to 0.93). This diel variability in K_d can be intuitively understood if we imagine the situation when a light beam is vertically incident on a nonscattering medium. In such a situation K_d would be equal to the absorption coefficient a. Again, if the medium were nonscattering but the light stream was not vertical, K_d would be equal to a/μ [*Kirk*, 1994a]. This results from the fact that for every meter of depth, the photons would travel a distance of $1/\mu$. A similar effect is also present in the scattering waters, and it seems logical to expect the measured K_d values to be inversely proportional to μ (see *Stavn* [1981] for the derivation of exponential decay equations for various kinds of submarine light fields).

Note, however, that in contrast to K_d at shorter wavelengths, K_d at 665 and 683 nm increased by more than 50% when the solar altitude increased from about 17° to 60° (when μ increased from

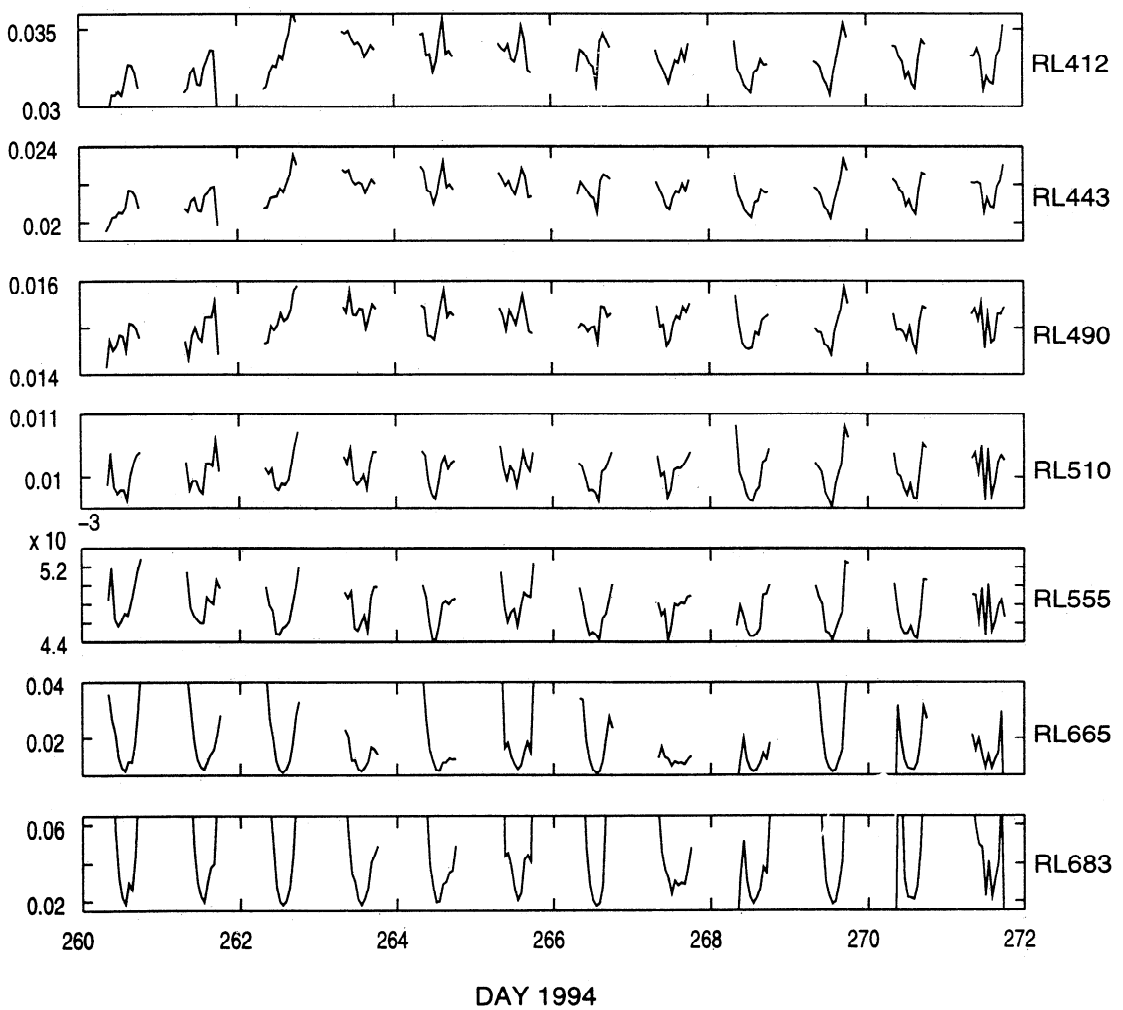

Figure 7. Time series of 15-m radiance reflectance (R_L, sr^{-1}) at seven wavelengths (412, 443, 490, 510, 555, 665, and 683 nm).

about 0.69 to 0.93). This pattern of daily K_d cycle at red wavelengths was probably an interesting manifestation of inelastic processes, i.e., Raman scattering [e.g., *Ge et al.*, 1995; *Waters*, 1995] and Sun-stimulated fluorescence [e.g., *Kiefer et al.*, 1989, *Chamberlin et al.*, 1990]. With decreasing Sun altitude (decreasing μ), less and less of the red light originating from the sea surface was able to reach the water column at the depths of our measurements and the relative number of Raman photons increased. Therefore inelastic processes increasingly dominated the light field at these wavelengths, and this is why the decrease in K_d with decreasing solar altitude (decreasing μ) was observed.

Thus far, we have considered daily changes of K_d as estimated from the irradiance measurements in selected wave bands of radiant energy spectrum. However, the most commonly

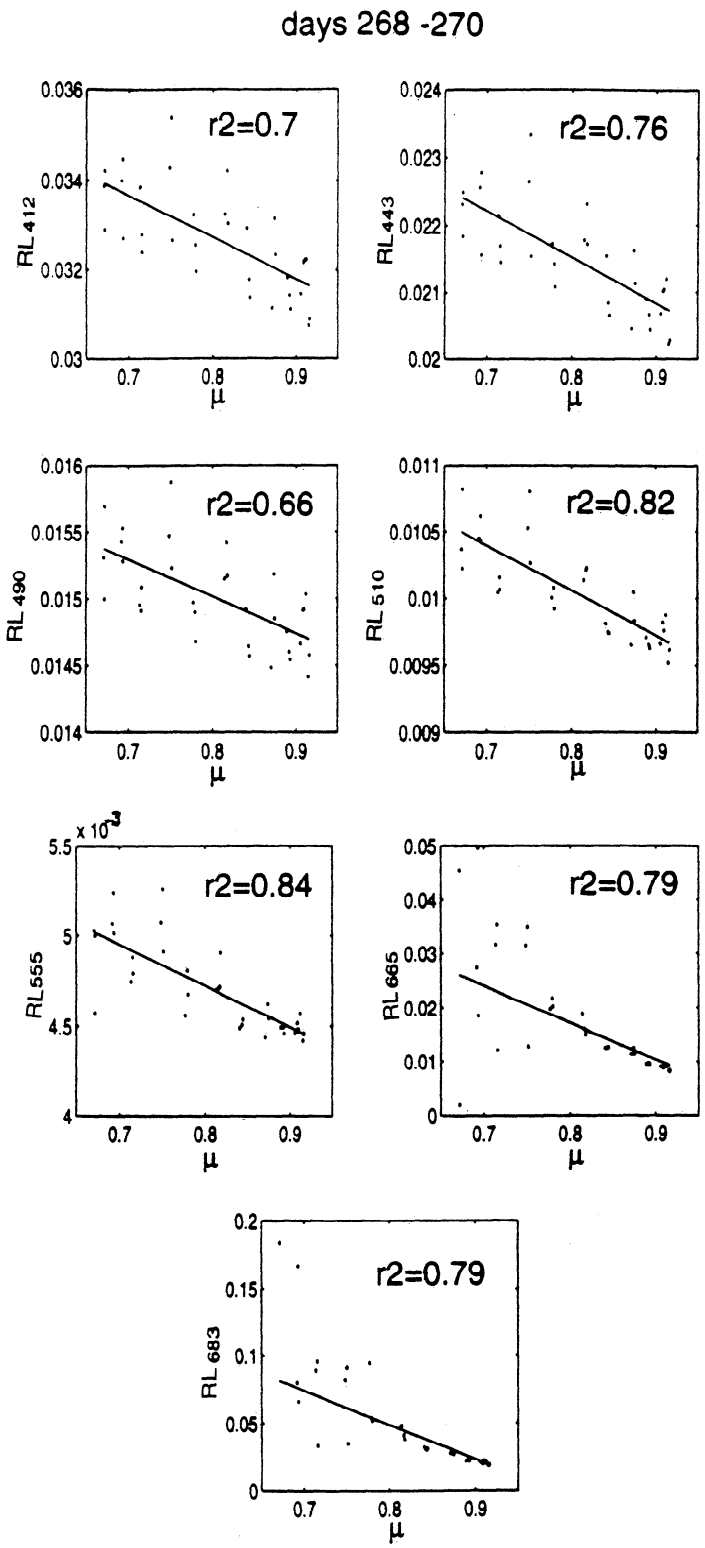

Figure 8. The dependence of 15-m radiance reflectance (R_L, sr^{-1}) on the cosine of the zenith angle of the direct solar beam in water (μ). The data points are shown for days 268-271.

measured in situ quantity for the bio-optical studies of the ocean has been a broadband measurement of photosynthetically available radiation PAR (visible spectrum range), either as a scalar (PAR_s) or downwelling irradiance (PAR_d). Scalar irradiance PAR_s is the total photon flux per unit area arriving at a point from all directions. This is more appropriate parameter for monitoring the availability of the radiant energy for photosynthesis than downwelling PAR. Often, when it is not possible to make the scalar irradiance measurement, it is replaced by the downwelling irradiance, due to the relative ease of this measurement. It may not always be realized that the downwelling irradiance is strongly influenced by the direction of the incident photons and depends on the angular structure of the light field. Thus replacing scalar PAR with downwelling PAR can lead to significant errors in productivity estimates and models. This fact is illustrated in Figure 5, which shows the diel variability of the ratio PAR_d/PAR_s at 15-m depth (Figure 5b), and the diel variability of the vertical attenuation coefficient for PAR_s (K_{PARs}, Figure 5a). The time series of the vertical attenuation coefficient for downwelling PAR (not shown) appear similar to the time series of K_{PARs}.

In Figure 6a we plotted the value of ratio PAR_d/PAR_s as a function of μ. Similarly, in Figure 6b, there is shown the K_{PARs} as a function of μ. From these plots one can see that the PAR_d/PAR_s ratio and K_{PARs} were changing by as much as 25% over a day, because of the change in the solar altitude. The error in the estimate of the total light available for photosynthesis could exceed 30% at low solar altitude (low μ), if scalar irradiance measurement was replaced by downwelling irradiance measurement.

We now discuss the daily variability of radiance reflectance R_L. The 15-m radiance reflectance estimated from radiometer time series data recorded on days 260-271 at seven wavelengths is shown in Figure 7. After that time period, the 15-m radiometers failed, probably due to a data acquisition software error. The important feature to note from Figure 7 is the tendency for R_L to generally follow the diel cycle. Note, however, that the diel variability of R_L in the blue wavelengths (415, 443, and 490 nm) seems to be less pronounced than the diel variability of R_L at the green and red part of the spectrum. The daily R_L cycle shown in Figure 7 seems to be sometimes obscured when clouds were covering the sky. The variability of chlorophyll concentration over the first three days of the deployment (days 260, 261, and 262), reflected in the 45-m fluorescence time series (Figure 2), could also have affected the reflectance observed at that time. Therefore for further discussion, we will focus on the reflectance data from days 268-270, that is, from a time period characterized by relatively clear skies and almost constant chlorophyll concentrations.

To check the dependence of R_L on solar altitude, the reflectance data from days 268 to 270 have been plotted in Figure 8 as a function of the cosine of the refracted solar zenith angle (μ). The statistical analysis performed on the data shown in Figure 4 indicates significant correlation between R_L and μ. We observed that on average, R_L recorded at 412-510 nm was higher by about 4-8% and at 555 nm was higher by about 11% at low solar altitude (low μ) than the R_L recorded at noon. Thus in the blue/green part of the light spectrum, R_L was much less sensitive to solar elevation than K_d. In contrast, R_L at 665 nm and 683 nm changed by more than 100%. This indicates that, similarly to K_d,

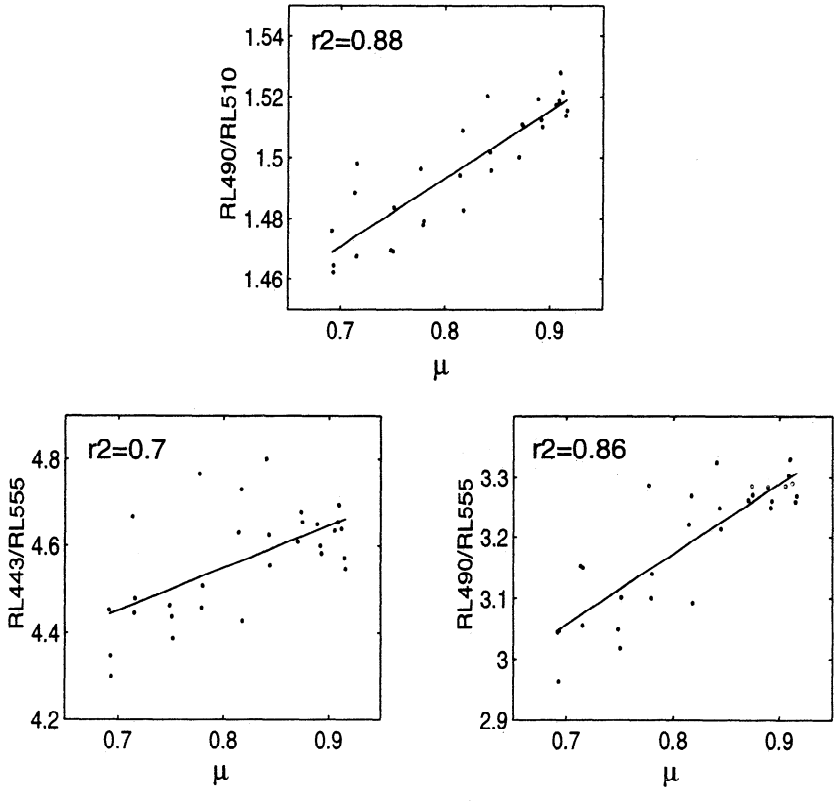

Figure 9. Examples of reflectance ratios as a function of μ.

the reflectance at red wavelengths is significantly affected by the fluorescence of phytoplankton cells and Raman scattering.

Remote-sensing techniques rely on the interpretation of reflectance and L_u ratios. Three examples of R_L ratios were plotted as a function of μ in Figure 9. The largest change was observed for the radiance reflectance ratio R_L490/R_L555 (about 8%). The ratios of upwelled radiance at selected wavelength are shown in Figure 10. Here the changes of the ratio were largest for L_u443/L_u555 and reached about 17%. From the comparison of Figures 9 and 10 it is clear that the R_L ratios are increasing with solar altitude (increasing with μ), while the L_u ratios are decreasing, and that the R_L ratios are in general changing less than L_u ratios. Note, however, that the maximum changes were observed for the ratios including L_u or R_L at 555 nm. It is expected that this increased variability of the ratios including L_u or R_L at 555 nm is due to the fact that the light field at 555 nm in the oligotrophic ocean is affected by Raman scattering.

It is not possible to compare quantitatively our observations with models, because the data necessary to run radiative transfer models such as the volume-scattering function, the absorption and scattering coefficients, and the incoming radiance distribution were not measured during our experiment. However, in order to understand better some of the observed patterns of the daily AOPs variability, it is useful to make a qualitative comparison between the data and the model simulation. Toward this goal we briefly present the results of calculations carried out with the Hydrolight 3.0 radiative transfer model [*Mobley*, 1989, 1994]. The model was run for an infinitely deep and optically homogenous ocean with a flat surface. The boundary conditions and the inherent optical properties of the oceanic case 1 waters were modeled using the library of subroutines provided with the Hydrolight, assuming chl *a* concentration of 0.1 mg m^{-3} and incoming radiance for a clear maritime sky. The model was run for the idealized situation with no inelastic processes affecting the light field and for the situation which included Raman scattering and chlorophyll fluorescence. The Raman wavelength redistribution function used in the model is described by Mobley [1994], but for the quick evaluation of the source wavelengths supplying Raman photons note that according to the model, photons with λ = 500 nm are shifted to about 600 nm, while photons with λ = 550 nm to about 680 nm.

The daily changes of K_d and R_L predicted with the model which included inelastic processes are summarized in Table 1. For a comparison similar results for the irradiance reflectance (R), another parameter often used in the ocean color studies, are also shown (recall that $R = E_u/E_d$, where E_u is the upwelling irradiance). For the consistency with the in situ data discussed before, the data included in Table 1 are based on reflectances at 15-m depth and K_d was estimated from E_d at 15- and 35-m depths. As can be seen the order of magnitude of daily K_d and R_L changes is similar in the model and in in situ data. According to the model, K_d and R are much more sensitive to the changes of solar altitude than the R_L. In agreement with our in situ observations, the model predicts a much larger daily amplitude of R_L changes for the red light than for the shorter wavelengths. The model also predicts an opposite pattern in the K_d daily cycle at 665 and 683 nm, in comparison to the K_d daily cycle at shorter wavelengths. A comparison of the model simulations with and

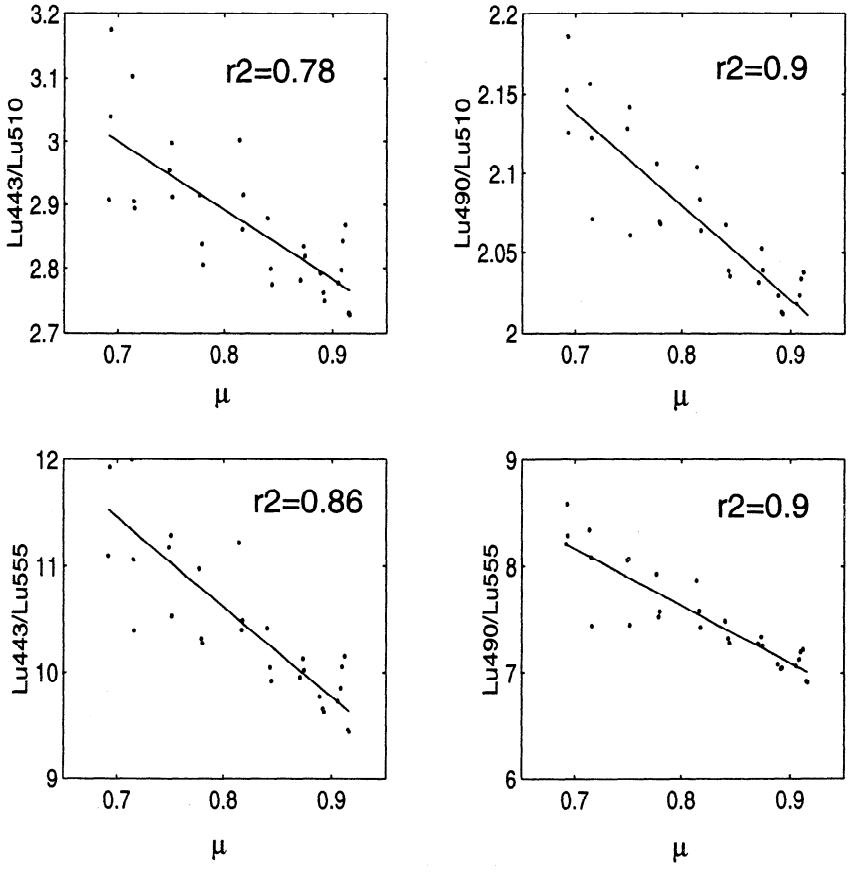

Figure 10. Examples of L_u ratios as a function of μ.

Table 1. Changes of the Vertical Attenuation Coefficient for Downwelling Irradiance (K_d), Irradiance Reflectance ($R = E_u/E_d$), and Radiance Reflectance ($R_L = L_u/E_d$) Corresponding to the Solar Altitude Decreasing from 60° to 10° (i.e. Cosine of the Refracted Solar Zenith Decreasing From 0.93 to 0.67).

	Kd	E_u/E_d	L_u/E_d
415 nm	13.0%	12.0%	1.0%
445 nm	15.0%	14.6%	1.7%
490 nm	17.3%	18.1%	2.4%
510 nm	17.1%	20.6%	3.2%
555 nm	16.0%	24.7%	6.4%
665 nm	-29.6%	116.5%	100.0%
683 nm	-3.0%	23.0%	22.0%

The estimates are based on 15-m reflectances and K_d calculated from E_d at 15- and 35-m depths. The results are for the Hydrolight model simulation with Raman scattering and chlorophyll fluorescence and assuming clear sky conditions, wind speed of 0 m s^{-1}, and chl *a* concentration of 0.1 mg m^{-3}.

without inelastic processes (not shown here) indicates that both the large amplitude of daily R_L changes and the increase of K_d with Sun elevation at 665 and 683 nm are due to the fact that the light field at these wavelengths is influenced by inelastic processes, as will be explained later. In fact, a somewhat higher amplitude of R_L variability at green wavelengths (515 and 555 nm) than at blue wavelengths can be attributed to Raman scattering as well. Note, however, that the changes of R_L and K_d predicted by the model at 683 nm are smaller than those observed in situ. This discrepancy was likely due to the differences between the chl *a* concentration assumed in the model and that encountered in situ, including the fact that the vertical structure of the chl *a* concentration present in the real ocean was not simulated by the model. At 683 nm the light field is affected strongly by the chlorophyll fluorescence; therefore the results of the model calculations are quite sensitive to the assumed chl *a* concentration. Also, the wind-blown sea surface effects not included in the model are expected to increase the in situ variability of AOPs with sun elevation, especially at low solar altitude (low μ).

The model results allow us to illustrate qualitatively the diel cycle of the vertical attenuation coefficient and reflectances in the light field affected by inelastic processes. The vertical profiles of K_d, R, and R_L at 665 nm obtained from the model simulations are shown in Figure 11. In the top of the water column the contribution of inelastically scattered light is negligible compared to the solar light coming from the sea surface. At depth we can distinguish a "transition zone" where inelastic scattering becomes gradually more prevailing; therefore an increase in reflectances and a decrease in K_d are observed. Finally, at even greater depths, the light field is always dominated by the light originating from inelastic processes. The exact vertical distribution of K_d and reflectances depends, for example, on the vertical distribution of the light at excitation and emission wavelengths and inherent optical properties of the water. However, in general, at lower Sun altitudes (lower μ), less solar irradiance penetrates to a given depth than at higher Sun altitudes (higher μ). Therefore the influence of inelastic scattering on K_d and reflectances becomes significant at shallower depths for the lower Sun altitudes (lower μ) than for the higher Sun altitudes (higher μ). As a result, when the instrument is placed at a fixed depth within the "transition zone," the decrease in K_d and the increase in reflectances will be observed when the Sun altitude is decreasing (decreasing μ).

In summary, the results presented in this paper demonstrate that under sunny sky conditions, the AOPs in the surface waters of the oligotrophic ocean are influenced by the Sun elevation. We observed that at the blue/green wavelengths the vertical attenuation coefficient K_d was much more sensitive to changes in solar elevation than the radiance reflectance R_L. At 665 and 683 nm the observed daily patterns of K_d and R_L resulted from the fact that the light field was significantly influenced by inelastic scattering. The daily changes of radiance and reflectance ratios used in ocean color studies were largest for the ratios involving L_u or R_L at green wavelengths (515 and 555 nm), also a result of inelastic scattering. Interestingly, *Smith et al.* [1991] carried out similar optical measurements from a mooring platform located in the Sargasso Sea and found that K_d did not display a significant

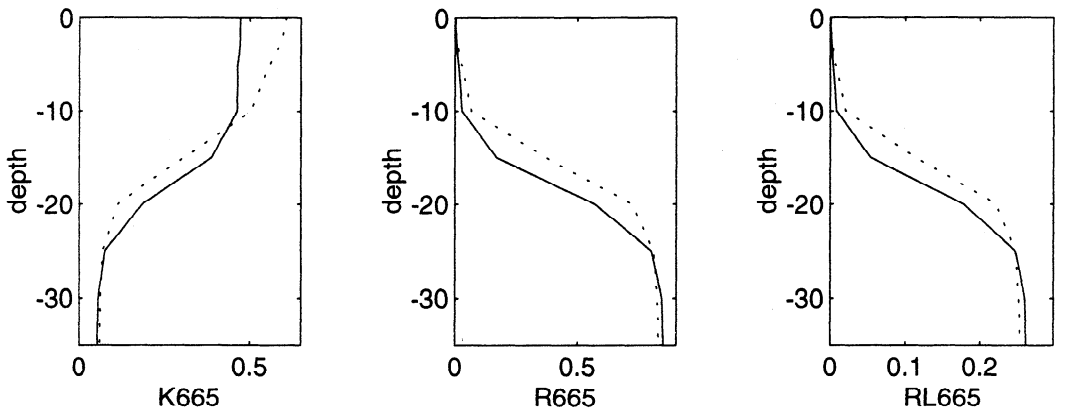

Figure 11. Vertical profiles of K_d (m^{-1}), irradiance reflectance (R, nondimensional), and radiance reflectance (R_L, sr^{-1}) at 665 nm obtained from the model simulation. Solid and dotted lines are for the solar altitude of 60° and 10°, respectively (cosine of the refracted solar zenith equal to 0.93 and 0.67, respectively).

diurnal variability in response to changes of solar altitude. We believe that the differences in the effects from variable Sun altitude observed in both experiments can be reasonably well explained. First, Smith et al. data were characterized by a relatively larger temporal variability of chl *a* concentration in the water than was observed during our experiment, and probably the relevant variability of IOPs dominated the variability of K_d. Second, the amplitude of daily K_d changes induced by solar altitude is expected to decrease with optical depth, i.e., when the light field approaches asymptotic radiance distribution. Note that radiometers were located at 33- and 52-m depths in the experiment described by Smith et al. and at 15- and 35-m depths in our experiment.

Although our data illustrate the dependence of AOPs on Sun altitude on a daily timescale, similar relationships are expected to be of importance on a seasonal scale and with latitude. For example, at the geographical position of our mooring, the solar altitude at noon in the summer can reach about 80°, while in the winter it can be as low as 35°, which correspond to μ being equal to 0.99 and 0.79, respectively.

Acknowledgments. This work was supported by NASA grant NAGW-3949 and NSF Oceanographic Technology and Interdisciplinary Coordination Program grant OCE-9415667, both awarded to T. Dickey and M. Stramska. The mooring hardware and telemetry have been funded by ONR Contract N00014-94-1-0346 to D. Frye. We thank colleagues from the Ocean Physics Group USC and in the BATS program for their outstanding dedication to collecting the data presented here. Special thanks are due to Derek Manov (UCSB), Liz Caporelli (BBSR), and Isabelle Taupier-Letage (CNRS, France) for their assistance with many aspects of the field work. We also thank the WHOI mooring team led by John Kemp, crew, marine technicians, and master of the *Weatherbird II* for their commitment to conducting the mooring operations. The Hydrolight model was made available by Curtis Mobley. Comments from two anonymous reviewers are appreciated.

References

Baker, K., and R. C. Smith, Quasi-inherent characteristics of the diffuse attenuation coefficient for irradiance, *Proc. SPIE Int. Soc. Opt. Eng.*, *208*, 60-63, 1979.

Chamberlin, W. S., C. R. Booth, D. A. Kiefer, J. H. Morrow, and R. C. Murphy, Evidence for a simple relationship between natural fluorescence, photosynthesis and chlorophyll in the sea, *Deep Sea Res., Part A*, *37*, 951-973, 1990.

Dera, J., and H. Gordon, Light field fluctuations in the photic zone, *Limnol. Oceanogr.*, *13*, 697-699, 1968.

Dickey, T. D., J. Marra, M. Stramska, C. Langdon, T. Granata, A. Plueddemann, R. Weller, and J. Yoder, Bio-optical and physical variability in the subarctic North Atlantic Ocean during the spring of 1989, *J. Geophys. Res.*, *99*, 22,541-22,556, 1994.

Ge, Y., K. J. Voss, and H. Gordon, In situ measurements of inelastic light scattering in Monterey Bay using solar Fraunhofer lines, *J. Geophys. Res.*, *100*, 13,227-13,236, 1995.

Gordon, H. R., Dependence of the diffuse reflectance of natural waters on the sun angle, *Limnol. Oceanogr.*, 34, 1484-1489, 1989.

Gordon, H. R., and A. Morel, *Remote Assessment of Ocean Color for Interpretation of Satellite Visible Imagery*, Coastal Estuarine Stud., vol. 4, edited by R. T. Barber, C. K. Mooers, M. J. Bowman, and B. Zeitzschel, 114 pp., AGU, Washington D.C., 1983.

Gordon, H. R., O. B. Brown, and M.M. Jacobs, Computed relationships between the inherent and apparent optical properties of a flat, homogenous ocean, *Appl. Opt.*, *14*, 417-427, 1975.

Jerlov, N. G., *Marine Optics*, Elsevier, New York, 1976.

Kiefer, D. A., and R. A. Reynolds, Advances in understanding phytoplankton fluorescence and photosynthesis, in *Primary Productivity and Biogeochemical Cycles in the Sea*, edited by P. G. Falkowski and A. Woodhead, pp. 155-174, Plenum, New York, 1992.

Kiefer, D. A., W. S. Chamberlin, and C. R. Booth, Natural fluorescence of chlorophyll a: Relationship to photosynthesis and chlorophyll concentration in the western South Pacific gyre, *Limnol. Oceanogr.*, *34*, 868-881, 1989.

Kirk, J. T. O., Dependence of relationship between inherent and apparent optical properties of water on solar altitude, *Limnol. Oceanogr.*, *29*, 350-356, 1984.

Kirk, J. T. O., Volume scattering function, average cosines, and the underwater light field, *Limnol. Oceanogr.*, *36*, 455-467, 1991.

Kirk, J. T. O., *Light and photosynthesis in Aquatic Ecosystems*, 2nd ed., 509 pp., Cambridge Univ. Press., New York, 1994a.

Kirk, J. T. O., Estimation of the absorption and the scattering coefficients of natural waters by use of underwater irradiance measurements, *Appl. Opt.*, *33*, 3276-3278, 1994b.

Kirk, J. T. O., Characteristics of the light field in highly turbid waters: A Monte Carlo study, *Limnol. Oceanogr.*, *39*, 702-706, 1994c.

Michaels A. F., et al., Seasonal patterns of ocean biogeochemestry at the US- JGOFS Bermuda Atlantic Time Series study site, *Deep Sea Res.*, Part I, *41*, 1013-1038, 1994.

Mobley, C. D., A numerical model for the computation of radiance distribution in natural waters with wind-roughened surfaces, *Limnol. Oceanogr.*, *34*, 1473-1483, 1989.

Mobley, C. D., *Light and Water: Radiative Transfer in Natural Waters*, 592 pp., Academic, San Diego, Calif., 1994.

Morel, A., and B. Gentilli, Diffuse reflectance of oceanic waters: Its dependence on Sun angle as influenced by the molecular scattering contribution, *Appl. Opt.*, *30*, 4427-4438, 1991.

Morel, A., and B. Gentilli, Diffuse reflectance of oceanic waters, II, Bidirectional aspects, *Appl. Opt.*, *32*, 6864-6879, 1993.

Morel, A., and L. Prieur, Analysis of variations in ocean color, *Limnol. Oceanogr.*, *22*, 709-722, 1977.

Mueller, J. L., and R. W. Austin, Ocean optics protocols, edited by S. B. Hooker and E. R. Firestone, *NASA Tech Memo. 104566*, vol. 5, 45 pp., 1992.

Mueller, J. L., J. McLean, and B. C. Johnson, The first SeaWiFS intercalibration round-robin experiment, SIRREX-1, edited by S. B. Hooker and E. R. Firestone, *NASA Tech. Memo. 104566*, vol. 14, 58 pp., 1993.

Siegel, D.A, D. Konnoff, M. C. O'Brien, J. Sorensen, and E. Fields, BBOP Sampling and Data Processing Protocols, technical report, U. S. JGOFS Plann. and Coord. Off., Woods Hole Oceanogr. Inst., Woods Hole, Mass., 1995.

Smith, R. C., and K. S. Baker, Oceanic chlorophyll concentrations as determined by satellite (Nimbus-7 coastal zone color scanner), Mar. Biol., Berlin, 66, 269-279, 1982.

Smith, R. R., K. J. Waters, and K. S. Baker, Optical variability and pigment biomass in the Sargasso Sea as determined using deep-sea optical mooring data, *J. Geophys. Res.* , *96*, 8665-8686, 1991.

Stavn, R. H., Light attenuation in natural waters: Gershun's Law, Lambert-Beer Law, and the mean light path, *Appl. Opt., 20*, 2326-2327, 1981.

Stramska, M., T. D. Dickey, J. Marra, A. Plueddemann, C. Langdon, and R. Weller, Bio-optical variability associated with phytoplankton dynamics in the North Atlantic Ocean during spring and summer of 1991, *J. Geoph. Res.* , *100*, 6605-6619, 1995.

Waters, K. J., Effects of Raman scattering on the water-leaving radiance, *J. Geophys. Res.*, *100*, 13,151-13,161, 1995.

Zaneveld, J. R., J. C. Kitchen, A. Bricaud, and C. C. Moore, Analysis of in situ spectral absorption meter data, *Proc. SPIE Int. Soc. Opt. Eng.*, *1750*, 187-200, 1992.

D. Frye, Woods Hole Oceanographic Institution, Woods Hole, MA 02543.

M. Stramska, Hancock Institute for Marine Studies, University of Southern California, Los Angeles, CA 90084-0373. (e-mail: stramska@usc.edu)

(Received November 21, 1996; accepted January 31, 1997.)